leukocyte images in conjunction with either traditional bone images or with bone marrow images can reduce the number of false-positive results. The leukocyte/marrow technique has been reported to be the more accurate procedure, however, and the results in this series are in agreement with this observation (*9*).

CONCLUSION

Although we cannot estimate the frequency with which it occurs, our data demonstrate, as have previous investigations, that uptake of labeled leukocytes does occur in the uninfected Charcot joint. Moreover, this activity does not merely reflect "inflammation"; rather, it represents areas of hematopoietically active marrow, albeit atypical in location, which may be a response to or, perhaps, part of the inflammation, bony destruction and bony remodeling that are part of this entity. Finally, our data illustrate that combined leukocyte/marrow imaging is useful for determining whether or not infection is present in a Charcot joint and that this technique is superior to both leukocyte and three-phase bone scintigraphy, alone or in combination, for this purpose.

REFERENCES

1. Schumacher HR Jr. Secondary osteoarthritis. In: Moskowitz RW, Howell DS, Goldberg VM, Mankin HJ, eds. *Osteoarthritis: diagnosis and management*. Philadelphia: W. B. Saunders; 1984:235–264.
2. Sanders LJ, Frykberg RG. Charcot foot. In: Levin ME, O'Neal LW, Bowker JH, eds. *The diabetic foot*. St. Louis: Mosby; 1993:149–180.
3. Park H-M, Wheat JL, Siddiqui AR, et al. Scintigraphic evaluation of diabetic osteomyelitis: concise communication. *J Nucl Med* 1982;23:569–573.
4. Maurer AH, Millmond SH, Knight LC, et al. Infection in diabetic osteoarthropathy: use of indium-labeled leukocytes for diagnosis. *Radiology* 1986;161:221–225.
5. Schauwecker DS, Park HM, Burt RW, Mock BH, Wellman HN. Combined bone scintigraphy and indium-111 leukocyte scans in neuropathic foot disease. *J Nucl Med* 1988;29:1651–1655.
6. Seabold JE, Flickinger FW, Kao SCS, et al. Indium-111-leukocyte/technetium-99m-MDP bone and magnetic resonance imaging: difficulty of diagnosing osteomyelitis in patients with neuropathic osteoarthropathy. *J Nucl Med* 1990;31:549–556.
7. Schauwecker DS. Differentiation of infected from noninfected rapidly progressive neuropathic osteoarthropathy. *J Nucl Med* 1995;36:1427–1428.
8. Palestro CJ, Kim CK, Swyer AJ, Capozzi JD, Solomon RW, Goldsmith SJ. Total hip arthroplasty: periprosthetic ^{111}In-labeled leukocyte activity and complementary ^{99m}Tc sulfur colloid imaging. *J Nucl Med* 1990;31:1950–1955.
9. Palestro CJ, Swyer AJ, Kim CK, Goldsmith SJ. Infected knee prosthesis: diagnosis with In-111-leukocyte, Tc-99m-sulfur colloid and Tc-99m-MDP imaging. *Radiology* 1991;179:645–648.
10. Palestro CJ, Roumanas P, Swyer AJ, Kim CK, Goldsmith SJ. Diagnosis of musculoskeletal infection using combined In-111-labeled leukocyte and Tc-99m sulfur colloid marrow imaging. *Clin Nucl Med* 1992;17:269–273.
11. Reimer G, Tan EM. Systemic sclerosis (scleroderma) and mixed connective tissue disease. In: Lachmann PJ, Peters K, Rosen FS, Walport MJ, eds. *Clinical aspects of immunology*, 5th ed. Boston, Blackwell Scientific Publications; 1993:1241–1258.
12. Thakur ML, Lavender JP, Arnot RN, Silvester DJ, Segal AW. Indium-111-labeled autologous leukocytes in man. *J Nucl Med* 1977;18:1014–1021.
13. Beltran J, Campanini DS, Knight C, McCalla M. The diabetic foot: magnetic resonance imaging evaluation. *Skeletal Radiol* 1990;19:37–41.
14. Fineman D, Palestro CJ, Kim CK, et al. Detection of abnormalities in febrile AIDS patients with In-111-labeled leukocyte and Ga-67 scintigraphy. *Radiology* 1989;170: 677–680.
15. Palestro CJ, Schultz BL, Horowitz M, Swyer AJ. Indium-111-leukocyte and gallium-67 imaging in acute sarcoidosis: report of two patients. *J Nucl Med* 1992;33:2027–2029.
16. Geratz JD, Pryzwanski KB, Schwab JH, Anderle SK, Tidwell RR. Suppression of streptococcal cell-wall induced arthritis by a potent protease inhibitor, bis(5-amidino-2-benzimidazolyl) methane. *Arthritis Rheum* 1988;31:1156–1164.
17. Hayashida K, Ochi T, Fujimoto M, et al. Bone marrow changes in adjuvant-induced and collagen induced arthritis. *Arthritis Rheum* 1992;35:241–245.
18. Carrington JL, Reddi AH. Parallels between development of embryonic and matrix-induced endochondral bone. *Bioassays* 1991;13:403–408.
19. Burwell RG. The function of bone marrow in the incorporation of a bone graft. *Clin Orthop Rel Res* 1985;200:125–141.
20. Paley D, Young MC, Wiley AM, Fornasier VL, Jackson RW. Percutaneous bone marrow grafting of fractures and bony defects. An experimental study in rabbits. *Clin Orthop Rel Res* 1986;208:300–312.
21. Connolly JF. Injectable bone marrow preparations to stimulate osteogenic repair. *Clin Orthop Rel Res* 1995;313:8–18.

Signal-Enhancing Switched Protocols to Study Higher-Order Cognitive Tasks with PET

Jorge J. Moreno-Cantú, David C. Reutens, Christopher J. Thompson, Robert J. Zatorre, Denise Klein, Ernst Meyer and Michael Petrides

Department of Neurology and Neurosurgery, Neuropsychology/Cognitive Neuroscience Unit and McConnell Brain Imaging Centre, Montreal Neurological Institute, McGill University, Montreal, Quebec, Canada

We tested the effectiveness of a switched protocol when it is used to detect signals that result from the study of a higher-order cognitive task with PET. Using language tasks that have been studied extensively in our laboratories, we compared the signal-to-noise ratio (S/N) and statistical significance of the activation signals detected in PET images of regional cerebral blood flow (rCBF), obtained using a standard activation protocol, and of activity concentration, obtained using a switched protocol. **Methods:** Four volunteers were studied with PET while they were performing synonym-generation and word-repetition tasks (activation and baseline tasks, respectively). Each volunteer had three activation/baseline and three baseline/activation scans. Data for each scan were collected in two frames (60 and 120 sec long). During the first 60 sec, data were collected using a standard activation protocol. Subjects then switched tasks, and acquisition continued for 120 sec. Two images were obtained from each scan: an rCBF image using the first frame and an activity-concentration image using both frames. Images were transformed into Talairach space, subtracted and averaged within and across subjects. Parametric t-statistic images were generated for each protocol, and the magnitude and significance of the activation signals yielded by the two acquisition methods were compared. **Results:** All the activation foci detected using measurements of rCBF were detected when the switched protocol was used; this protocol, in addition, yielded better S/N values. The cognitive component introduced by task-switching in switched protocols did not yield extra statistically significant foci. In single subjects, the average improvement in the signal significance from regions of activation, at a 95% confidence level, was between 6% and 25%. When scans were averaged across subjects, the switched protocol yielded improvements in signal statistical significance of up to 38%. **Conclusion:** We present evidence suggesting that switched protocols can be used to study higher-order cognitive tasks and that they yield activation foci with S/N values that are greater than those of equivalent foci detected using an rCBF protocol. Switched protocols appear to be easy to apply to the testing of higher-order cognitive functions. However, the extra cognitive requirement of switching tasks during data acquisition may be a limiting factor when switched protocols are used to study memory processes.

Key Words: PET; switched protocols; activation studies; oxygen-15-water; cerebral blood flow

J Nucl Med 1998; 39:350–356

Received May 31, 1996; revision accepted Apr. 15, 1997.

For correspondence or reprints contact: Christopher J. Thompson DSc, Montreal Neurological Institute, Room 798, 3801 University Street, Montreal, Quebec, Canada H3A 2B4.

PET activation studies, using bolus injections of $H_2{}^{15}O$, have become a powerful and widely used tool for identifying and localizing cognitive function (*1*). By imaging parameters such as regional cerebral blood flow (rCBF) or tissue activity concentration, PET images provide quantitative or qualitative measurements of brain function through the identification of the neuronal foci involved in the execution of cognitive tasks (*2–4*). Identification of brain function using bolus injections of $H_2{}^{15}O$ is accomplished by comparing measurements that are acquired while the brain executes different tasks. Frequently, signals from brain regions that are activated when the brain is performing higher-order cognitive tasks have magnitudes similar to the noise present in PET images. This makes it necessary to use techniques that are designed to increase the signal-to-noise ratio (S/N) of PET images. Averaging of subtracted images is one such technique that has been used successfully for the study of cognitive function with PET (*5*). The effectiveness of this technique in reducing image noise is ultimately constrained by the total number of counts compounded in the final averaged image. The total number of image-forming counts detected in a scan depends on:

1. The scanner's sensitivity, which is intrinsic to the manufacturer's design;
2. The total injected dose, which is limited by the maximum permissible dose administered to volunteers and patients; and
3. The scan length, which is dependent on whether quantitative or qualitative assessment of brain function is required.

Scans providing quantitative measurements of rCBF are acquired for 40–60 sec after the tracer arrives in the brain (*6,7*), whereas scans optimizing the S/N are typically 60–90 sec long (*3,4*).

One technique that enhances the S/N of activation foci, by manipulating the scan length, is the switched protocol (*8*). When switched protocols are used, the difference between activity concentration in activation and baseline regions is maintained for over 3 min. This allows the use of scanning times that are longer than those used in standard activation protocols measuring rCBF or activity concentration. In switched-protocol scans, subjects execute the task under study until the total concentration of tracer in the brain reaches a maximum. Subjects then switch task execution from activation to baseline or vice versa, and the new task is performed until data acquisition ends. Thus, in an activation scan, subjects start executing the activation task and then switch to execute the baseline task. The opposite order is followed during baseline scans. Switching tasks during data acquisition is performed to reduce or accelerate tracer washout from activation and baseline foci. In the activation scans, washout in foci used for the execution of the activation task is reduced after total brain activity concentration peaks, whereas washout in foci activated during the execution of the baseline task is accelerated. Similarly, in the baseline scans, washout is reduced in foci used for the baseline task, whereas washout in foci used during the activation task is accelerated. The effects of using a standard or a switched protocol on the accumulation of tracer in a gray-matter region under activation and baseline conditions are shown in Figure 1. Using a typical measured input-function (*9*) and a compartmental model (*10*), we simulated the idealized kinetics of $H_2{}^{15}O$ in the brain when standard and switched protocols are used. Figure 1A shows the input function, and Figure 1B shows the resulting time-activity curves for a period of 3 min. For the simulations, blood flows in gray matter in baseline and activation states were 65 $ml \cdot min^{-1} \cdot 100\ g^{-1}$ and 91 $ml \cdot min^{-1} \cdot 100\ g^{-1}$ (a 40% activation), respectively, and the partition coefficient was set to 0.9 $ml \cdot g^{-1}$. The mean whole-brain time-activity curve was simulated using a blood-flow value of 50 $ml \cdot min^{-1} \cdot 100\ g^{-1}$ and individual time-activity curves were normalized by the value for whole-brain radioactivity integrated over a 3-min period. As seen in Figure 1B, at the beginning of the 3-min period, the standard protocol yields a relative (activation − baseline) accumulation of tracer as a consequence of the difference in flow between the activation and baseline states (uptake phase). However, soon after that, the difference in tissue activity between activation and baseline states decreases as a result of the higher unidirectional transfer of tracer from brain to blood (washout phase) that is introduced by maintaining the difference in flow when the arterial concentration of tracer is low (Fig. 1). Figure 1B also shows that, when a switched protocol is used, the difference between the time-activity curves is maintained throughout the 3-min period. Because the task switch was simulated at 60 sec, the baseline and activation time-activity curves for the two protocols are the same during the first minute. However, in the switched protocol, after the tasks are switched, the activation state (high flow) is changed to a baseline state (low flow), and vice versa. This has the effect of reducing flow in the initially activated region at a time when the arterial concentration of tracer is low so that the transfer of tracer from brain to blood (washout) is decreased. Because the opposite also occurs in the region when it was initially set to a baseline state, the difference between the activation and baseline time-activity curves is prolonged.

The simulations have been verified by detailed experimental observations of $H_2{}^{15}O$ kinetics in standard and switched activation scans, up to 4 min long (*8,11*). Volkow et al. (*11*) studied experimentally the correlation of the scan length and the timing of stimulus presentation with the signals from activation or baseline brain regions in scans up to 3 min long, using a standard activation protocol. They found that the difference between signals from activation and baseline regions was greatest during the first 40 sec after the arrival of tracer in the brain (uptake phase), and after the uptake phase, the difference decreased. Cherry et al. (*8*) used computer simulations of a compartmental model, as well as experimental measurements, to study tracer concentration in activation and baseline regions when using standard and switched protocols in scans up to 4 min long and for different switching times. Using simple visual and primary motor stimuli as activation tasks, they observed that the difference between activation and baseline signals was maintained for over 3 min when a switched protocol was used and for less than 2 min when a standard activation protocol was used. They also presented evidence suggesting that the optimal switching time was between 50 sec and 80 sec after bolus injection.

As described above, the effectiveness of using switched protocols to study brain function has been demonstrated with simple visual and motor stimuli (*8*); however, their effectiveness in the study of higher-order cognitive functions has not been investigated.

In this experiment, we analyze the effectiveness and applicability of switched protocols for the study of higher-order cognitive tasks. This is important because the potential improvements to the S/N of PET activation images of higher-order cognitive function would facilitate the use of PET to study such processes in single subjects. Testing the use of switched protocols to study higher-order cognitive functions is necessary because:

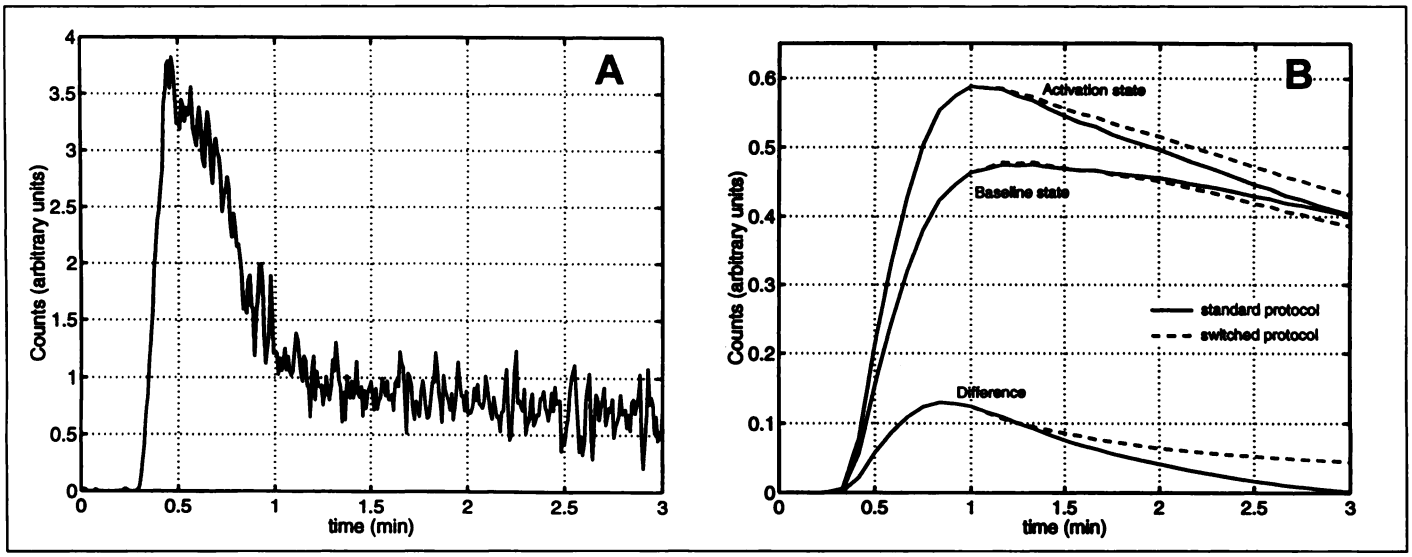

FIGURE 1. Computer simulations of the accumulation of $H_2{}^{15}O$ in a gray-matter region under activation and baseline conditions when standard and switched protocols are used. (A) Measured input function (*9*) used in the simulations. (B) Activation and baseline time-activity curves yielded by the standard and switched protocols. The bottom curves show the difference in activity-concentration between activation and baseline states in each of the protocols. Note how the switched protocol prolongs and enhances the difference between states during the second half of the simulated period.

1. The use of a switched protocol adds an extra cognitive component to the task being studied (subjects have to change tasks when presented with a given cue), and the extra cognitive component may lead to the detection of activation foci not related to the task under analysis;
2. The effect of neuropsychological habituation on task execution (*12,13*), enhanced by the long scanning times used in switched protocols, is likely to compete with the S/N gains resulting from decreased image noise; and
3. The greater complexity of implementing a switched protocol is likely to discourage its use for the routine study of cognitive function in normal volunteers and neurological patients.

In this experiment, a switched protocol was tested by using two language tasks that were extensively studied in our laboratories with PET and that have been found to consistently activate a specific group of brain regions (*14,15*).

MATERIALS AND METHODS

The tasks of generating synonyms and repeating words were studied in four healthy volunteers using the GE-Scanditronix PC-2048 15-slice PET scanner (*16*). The scans were performed in accordance with the ethical guidelines for PET studies of human subjects in effect at our institution. All subjects were right-handed and native English speakers (three men and one woman; mean age = 24 yr). The brain regions that were activated during synonym generation (activation task) were identified by subtracting PET images that were acquired during word repetition (baseline task). The studied tasks were as follows.

Activation and Baseline Tasks

For the activation task, English words were presented binaurally, every 4.2 sec, to the subjects. After hearing each word, the subjects had to generate a synonym and say it aloud (e.g., speak → talk, beverage → drink and so on). If a synonym was not found, they were told to say "pass." For the baseline task, words were presented to the subjects, as in the activation task, but in this case, subjects repeated each word aloud. The stimuli were matched, across scans, on a range of psycholinguistic parameters (e.g., length, syllable number, frequency and part of speech).

Scanning Conditions

During the execution of each task, the lights in the scanning room were dimmed, and the subjects kept their eyes closed. Subjects rehearsed both tasks a few minutes before starting the scanning sessions using word lists that were similar but not identical to those used in the scans. The stimuli used while scanning were never repeated, to minimize practice effects (*12*). Each subject was scanned six times, and each scan was performed using 40 mCi $H_2{}^{15}O$, administered intravenously as a 3-sec bolus. The maximum total activity we can administer to volunteers in compliance with ethical guidelines in effect at our institution is 240 mCi. The presentation of stimuli started when the bolus was injected, and data acquisition began once the tracer arrived in the brain. The length of the rCBF scans (and, therefore, the timing of task switching), as well as the procedure for the presentation of stimuli, were chosen to match the scanning parameters used in an rCBF PET activation experiment previously performed in our laboratories as part of a different study [Klein et al. (*14*)]. In that experiment, the synonym-generation task was studied in 12 subjects. Matching the scanning parameters allowed us to use the findings from that experiment as a reference for identifying activation foci in standard- and switched-protocol images obtained with the four-subject experiment discussed here.

Data Acquisition

Scans were acquired in two frames of 60 and 120 sec. During the first 60 sec, subjects performed the activation or baseline task. Then, the subjects heard the sound that they had been instructed to recognize as the cue prompting them to switch tasks (from activation to baseline or vice versa), and this task was executed for another 120 sec. Images were reconstructed with an 18-mm FWHM Hanning filter and were corrected for isotope decay and scattered events only. Images were not corrected for random events to maximize the S/N (*17*) (J. J. Moreno-Cantú and C. J. Thompson, *personal communication*, 1995). The filter size was selected to overcome the across-subject anatomical variability present in images after they are transformed into a common stereotaxic coordinate system (see below). In addition to the PET scans, each subject had an MRI scan that was coregistered with the PET data to facilitate the identification of the anatomical structures corresponding to the PET activation foci (*18–20*).

Data Analysis

The data were grouped to form rCBF images, using the first frame of each scan, and activity-concentration images, generated with the switched protocol after grouping the two frames of each scan. Parametric t-statistic images of the averaged subtracted rCBF and the averaged subtracted activity-concentration scans were generated using software developed in our laboratories. A detailed description of the statistical method used here has been described elsewhere (*21*). In brief, the parametric volume images were created as follows:

1. Individual scans were transformed into a stereotaxic coordinate system (*18,19*) and normalized to have a mean of 100;
2. Baseline scans were subtracted from the activation scans, and the resulting images were averaged;
3. A s.d. image of the subtracted scans included in the average was generated;
4. The pooled s.d. from all the voxels in the s.d. image was calculated; and
5. t values for voxels in the averaged image were calculated by dividing each voxel value by the pooled s.d. of the image and multiplying by the square root of the number of subtractions averaged.

Parametric images were then searched for peaks of activation. The statistical significance of the activation foci was determined from their associated pooled t-statistic voxel values using Gaussian random field theory (*21*). A focus was deemed statistically significant if the probability of being a false-positive was less than 5% ($t > 4.5$).

Foci: Identification and Functional Roles

Analysis of single- and across-subject rCBF data resulting from the synonym-generation experiments previously performed in our laboratories (*14,15*) suggests that a group of brain regions are activated when these types of lexical search-and-retrieval operations are performed. Thus, when auditory input and speech output are controlled for by subtracting word repetition from synonym generation, several distinct neuronal foci are activated. These are:

1. The left inferior frontal cortex (Brodmann's areas 45 and 47);
2. The left posterior dorsolateral frontal cortex (Brodmann's areas 9/46 and 8);
3. The left inferotemporal cortex (Brodmann's area 20);
4. The left posterior parietal cortex (Brodmann's area 7); and
5. The right cerebellar cortex.

Among these regions, the strongest and most consistently activated region is the left inferior frontal cortex, suggesting that this area may be specifically involved in lexical search-and-retrieval tasks (*12,14,15,22,23*). The left posterior dorsolateral frontal cortex is believed to be a part of a distributed neural circuit underlying certain aspects of working memory (*14,24*), whereas the left inferotemporal cortex is believed to be involved in the processing of words (*12,14*). The roles of the left posterior parietal and right cerebellar cortices are still unclear, although similar activations foci have been observed when subjects perform a wide range of lexical search operations (*12,14*).

The activation foci described above were localized in the single- and across-subject t-statistic images derived from the standard- and switched-protocol images. Foci across protocols were then compared based on:

1. Signal magnitude;
2. Statistical significance;
3. Spatial location; and
4. Signal-to-noise ratio.

RESULTS AND DISCUSSION

Activation Foci

Tables 1 and 2 show the location in Talairach coordinates (x,y,z), signal magnitude (m) and level of statistical significance (t) of the activation foci associated with the task of generating synonyms for single- and across-subject analyses, respectively.

The single-subject data in Table 1 were obtained by averaging the three activation − baseline pairs acquired from each subject. The switched protocol yielded activation foci of greater statistical significance than did the foci resulting from the rCBF protocol in 28 of the 36 regions of activation analyzed. We observed individual t-value increases of up to 73%. Because the t-value increases varied over a large range (which is expected because the single-subject analysis was based on the average of three subtractions), we evaluated whether the differences between rCBF- and switched-protocol t values were statistically significant. The significance of the improvements was determined using a paired comparison of small samples with 35 degrees of freedom. Because the foci analyzed were independent, the relative changes in t values can be considered to be a sample of a new random variable. Statistical analysis of this new sample suggests that the improvements are significant. Thus, at a 95% confidence level, the average improvement falls between 6% and 25%.

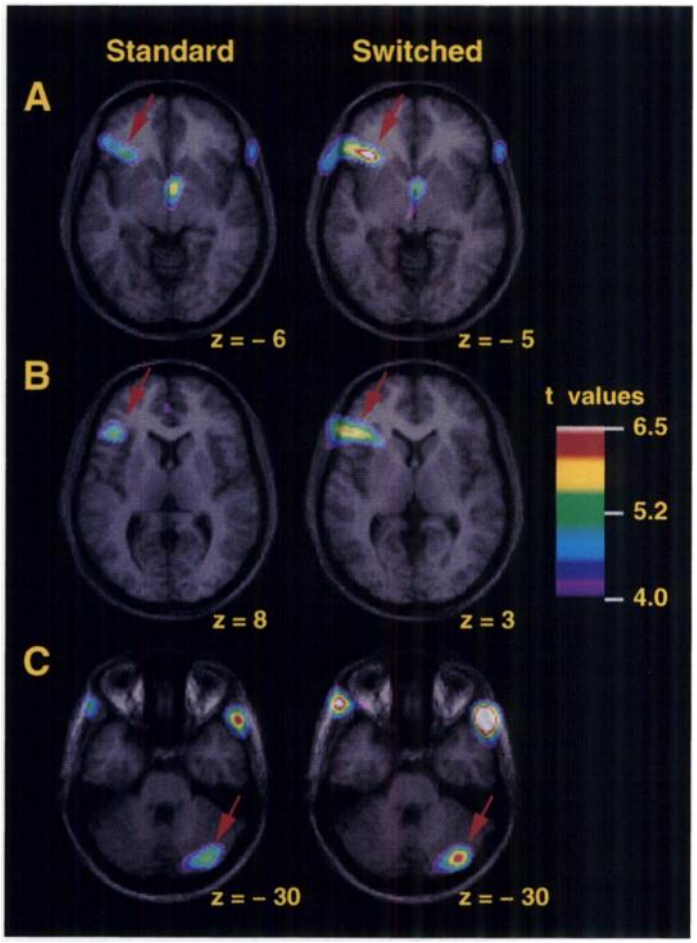

FIGURE 2. Comparison of rCBF- and switched-protocol t-statistic parametric PET images obtained from data averaged across subjects. Only foci identified as statistical significant by the rCBF protocol were used in the comparison. Nuclear MRI were superimposed on the parametric images in stereotaxic space to facilitate anatomic localization (*18–20*). (A and B) The left inferior frontal activations (Table 2, Foci 1 and 2, respectively), which are the most consistently activated regions during lexical search-and-retrieval tasks. (C) The right cerebellar activation (Table 2, Focus 9).

TABLE 1
Comparison of Regional Cerebral Blood Flow- and Switched-Protocol Activation Foci in Data Averaged within Subjects*

	rCBF protocol			Switched protocol			
	(x,y,z)	m	t	(x,y,z)	m	t	%Δt
Subject 1							
Left frontal ventrolateral	−40,36,−9	7.2	2.5	−25,20,−5	6.9	3.5	37.7
Left frontal ventrolateral	−54,28,6	5.9	2.1	−55,30,5	7.1	3.6	72.5
Left frontal dorsolateral†	—	—	—	—	—	—	—
Left frontal medial	1,20,53	8.9	3.1	3,22,53	5.1	2.6	−16.2
Left inferotemporal	−56,−54,−2	9.4	3.3	−49,−50,−7	4.7	2.4	−28.6
Left inferior posterior parietal‡	—	—	—	—	—	—	—
Occipital	10,−80,9	3.6	1.2	2,−86,8	4.2	2.1	72.6
Cerebellum vermis	3,−68,−18	9.7	3.4	4,−64,−18	9.4	4.7	38.8
Cerebellum right	29,−76,−35	11.1	3.9	32,−80,−35	8.2	4.1	5.9
Cingulate	7,43,29	4.9	1.7	3,41,27	5.6	2.8	64.0
Subject 2							
Left frontal ventrolateral	−31,25,−2	9.0	3.8	−34,24,−2	7.2	4.6	20.5
Left frontal ventrolateral	−38,25,6	7.7	3.2	−28,22,6	6.4	4.1	25.9
Left frontal dorsolateral	−26,16,30	3.6	1.5	−32,18,30	2.9	1.9	24.0
Left frontal medial	−42,17,51	7.6	3.2	−42,18,51	5.5	3.5	10.1
Left inferotemporal	−46,−33,−14	6.4	2.7	−48,−44,−14	5.0	3.2	17.0
Left inferior posterior parietal	−40,−49,54	5.6	2.4	−40,−47,56	2.7	1.7	−28.2
Occipital	−19,−82,−3	5.8	2.5	−9,−85,5	4.9	3.1	27.6
Cerebellum vermis	3,−78,−18	8.5	3.6	13,−78,−18	7.5	4.8	33.1
Cerebellum right	34,−66,−18	10.4	4.4	34,−69,−26	7.3	4.7	7.6
Cingulate	−5,30,36	7.0	3.0	−4,29,36	4.8	3.1	4.4
Subject 3							
Left frontal ventrolateral	−50,34,−12	9.03	3.5	−42,29,−5	6.90	4.12	18.1
Left frontal ventrolateral	−40,27,9	10.24	4.0	−47,24,3	7.87	4.70	18.7
Left frontal dorsolateral	−50,12,24	5.15	2.0	−46,13,24	3.40	2.03	2.0
Left frontal medial	−8,20,50	9.62	3.7	−5,22,50	7.15	4.27	14.8
Left inferotemporal	−64,−45,−11	9.83	3.8	−60,−49,−11	5.09	3.04	−20.0
Left inferior posterior parietal†	—	—	—	—	—	—	—
Occipital	11,−100,3	11.82	4.6	15,−99,−3	5.64	3.37	−26.3
Cerebellum vermis	−11,−64,−18	5.35	2.1	−7,−61,−18	5.86	3.50	69.1
Cerebellum right	35,−81,−30	11.15	4.3	39,−81,−30	7.70	4.60	6.7
Cingulate	3,41,36	13.99	5.4	−1,32,36	7.45	4.45	−17.7
Subject 4							
Left frontal ventrolateral	−46,30,−6	13.2	4.8	−42,27,−6	12.1	6.4	34.0
Left frontal ventrolateral†	—	—	—	—	—	—	—
Left frontal dorsolateral	−43,17,24	12.2	4.4	−47,15,24	5.6	3.0	−32.3
Left frontal medial	−13,34,48	9.6	3.4	−4,22,48	6.7	3.5	2.0
Left inferotemporal	−29,−64,−3	8.2	2.9	−34,−66,−3	8.6	4.6	55.3
Left inferior posterior parietal	−28,−63,44	6.5	2.3	−21,−62,44	4.9	2.6	11.6
Occipital	−8,−95,6	7.3	2.6	−9,−92,6	3.4	1.8	−30.9
Cerebellum vermis	7,−59,−18	8.5	3.0	−16,−74,−18	8.7	4.6	50.7
Cerebellum right	20,−83,−33	11.2	4.0	13,−68,−26	8.6	4.5	12.7
Cingulate	−7,41,33	7.1	2.6	−9,41,32	4.9	2.6	1.6

*The columns labeled "x,y,z" show the location, in Talairach space, of the activation foci; the columns labeled "m" and "t" show the magnitude and t value associated with each activation focus, respectively; and the column labeled %Δt shows the relative increase in focus t value yielded by the switched protocol
†Foci not found in subject.
‡Area not scanned in subject.

Table 2 shows the magnitude and significance level of the activation foci described in Table 1, when detected by averaging subtracted scans across subjects. The results from the synonym-generation study of Klein et al. (*14*) are shown in Table 2 as a reference only. Use of the switched protocol improved the statistical significance of the activation foci by an average of 14%. Improvements were observed in eight of the nine regions analyzed. One region, the left posterior parietal region (Focus 6), was not included in this comparison because it was not scanned in one of the subjects. The t value for Focus 7 decreased when the switched protocol was used; however, this focus was not statistically significant. All of the statistically significant foci were improved when the switched protocol was used (Fig. 2), and their mean improvement was 19%.

Analysis of the signal magnitudes (see Tables 1 and 2) shows that the normalized activation signals detected with the switched protocol were smaller than those measured with the rCBF protocol. All the magnitudes were obtained from the analysis of normalized datasets (see Materials and Methods). The decreases in signal magnitude are consistent with the simulated model because the normalized differences between activation and baseline regions, although maintained for a longer period when the switched protocol is used, become smaller than their rCBF-protocol counterparts. Nevertheless,

TABLE 2
Comparison of Regional Cerebral Blood Flow- and Switched-Protocol Activation Foci in Data Averaged Across Subjects*

	Klein et al. (*14*)			rCBF protocol			Switched protocol			
Focus	(x,y,z)	Brodmann area	t	(x,y,z)	m	t	(x,y,z)	m	t	%Δt
1	−42,39,−6	47	6.0	−43,34,−6	13.8	5.0	−36,27,−5	12.9	6.9	38
2	−46,27,12	45	4.83	−42,25,8	15.2	5.5	−40,25,3	10.8	5.8	6
3	−52,24,27	9/46	3.39	−44,13,24	5.23	1.9	−45,16,24	4.48	2.4	26
4	−3,22,54	8b†	3.11	−5,18,50	10.2	3.7	−3,20,50	7.83	4.2	12
5	−55,−40,−12	37/20	3.31	−56,−52,−11	7.99	2.9	−59,−52,−11	5.59	3.0	4
6	−38,−64,53‡	7	3.43	—	—	—	—	—	—	—
7	0,−92,6	17/18	3.63	7,−99,3	7.44	2.7	5,−87,8	4.85	2.6	−3
8	−4,−64,−24	Cerebellum	3.07	−3,−64,−18	10.2	3.7	−4,−61,−18	9.14	4.9	31
9	16,−86,−33	Cerebellum	3.76	35,−80,−30	15.4	5.6	36,−78,−30	11.7	6.3	14
10	1,42,30	24/32	3.47	9,48,36	10.7	3.9	−4,29,36	7.27	3.9	0

*The columns labeled "x,y,z" show the location, in Talairach space, of the activation foci; the columns labeled "m" and "t" show the magnitude and t value associated with each activation focus; and the column labeled %Δt shows the relative increase in focus t value yielded by the switched protocol. The focus identification numbers correspond to those shown in Table 1.

†Nomenclature after Petrides and Pandya (*25*).

‡Region not scanned in all subjects.

focus significance is enhanced because the image noise is decreased and the S/N is, therefore, increased. Table 3 shows estimates of the noise in the averaged subtracted images from each subject. The use of the switched protocol consistently decreased the image noise. The S/N gains yielded by the switched protocol could not be achieved by using a standard protocol in scans of similar length because, as previously explained, the difference in the signals from an activation and a baseline state when using a standard protocol diminishes (and may eventually become negative) at a faster rate than when a switched protocol is used.

It is important to note that the experiment of Klein et al. (*14*) is used as a reference because it was obtained from a larger sample size and, consequently, offers better statistical estimates. However, a comparison of t values between the study of Klein et al. (*14*) and the study shown here was not performed because the two experiments were acquired differently. In the Klein et al. (*14*) experiment, 12 subjects were scanned, and each subject had seven 34-mCi scans. However, only one synonym-generation scan and one word-repetition scan were acquired per subject. The t-statistic image of Klein et al. (*14*) was formed by averaging one subtracted image from each of the 12 subjects, whereas, in the experiment described here, the parametric image was formed by averaging three subtracted images from each of four subjects. Thus, the two experiments were affected differently by anatomical and functional intersubject variability, as well as by any practice-related effects introduced by task repetition.

The group of brain regions activated during the execution of the synonym-generation task and detected using measurements of rCBF also was detected when the switched protocol was used, which, in addition, yielded better S/N. Use of the switched protocol did not generate additional statistically significant foci. The cognitive component introduced by task-switching in switched protocols did not yield additional statistically significant foci, probably because task-switching was required in the activation and baseline tasks and, therefore, the activation foci introduced by this component would be canceled when the tasks were subtracted.

Changes in the Location of Foci Maxima

The coordinates (x,y,z) shown in Tables 1 and 2 indicate the location of the voxel of maximum value for each activation focus. The locations for equivalent foci across protocols were not identical. However, although foci identified in the switched-protocol images generally seemed to be smaller in spatial extent than those identified in the rCBF images, no significant differences were observed between the locations of equivalent foci across protocols. The mean difference between equivalent foci in single subjects was 7 mm. These variations in the location between equivalent foci can be explained by the statistical noise intrinsic to counting statistics because standard- and switched-protocol images are derived from different measurements (*26*) (J. J. Moreno-Cantú and C. J. Thompson, *personal communication*, 1995).

Practical Aspects of Implementing a Switched Protocol

Imaging cognitive function using a switched protocol is slightly more difficult than using a standard activation protocol because two tasks are executed per scan instead of only one. However, extra personnel are not required if the presentation of the stimuli and the switching signal are adequately organized. None of the scanned volunteers found the period of stimulation tiring. In fact, they reported that the reduced waiting periods between injections improved their level of alertness throughout the scanning session because the scans were longer and the period between injections is the same as in standard protocols. The subjects found it easy to switch tasks, and none reported difficulties remembering what task to switch to, although the type of stimulus materials presented before and after the switching signal were of a similar nature. Thus, based on our observations, switched protocols can be used routinely to study cognitive function in normal volunteers. In the paradigm tested here, we demonstrated that the S/N gains yielded by the switched protocol exceeded signal changes caused by task repetition. However, our paradigm required the use of novel stimuli only, and all the stimuli were different and uncorrelated to minimize a practice effect. Nevertheless, because using a switched protocol can triple or quadruple the number of times a cognitive task is performed, task habituation may be a problem in the study of some cognitive processes.

It is also important to note that acquisition of activity-concentration images using switched protocols does not impede the acquisition of rCBF images. Simultaneous acquisition of rCBF and activity-concentration switched-protocol images can be accomplished by simply acquiring data in two consecutive frames. The first frame, corresponding in length to that of an rCBF measurement, is used to collect data before task switching, whereas the data collected after task switching is stored in

TABLE 3
Noise Estimation

Subject	rCBF protocol Pooled s.d.*	Switched protocol Pooled s.d.*	Δ%†
1	4.96	3.43	−30.8
2	4.11	2.71	−34.1
3	4.48	2.90	−35.3
4	4.82	3.29	−31.7

*The pooled s.d. values shown are estimations of the image noise found across all intracerebral voxels. The values were calculated for each subject by comparing voxel magnitudes in individual subtracted images against mean voxel magnitudes obtained by averaging subtracted images within subjects (*21*).

†Percentage change in image noise yielded by the switched protocol.

a second frame. Activation foci can then be detected in the scans measuring blood flow by using only the first frame of each scan and in the activity-concentration scans by grouping the two frames within each scan. Nevertheless, this two-frame acquisition scheme will require twice the amount of computer disk space than do standard-activation protocols, and it will also double the image reconstruction time. The extra requirements should be considered, particularly when several subjects are scanned in one session.

Overall, three main disadvantages were identified when switched protocols were used to study cognitive paradigms. These are:

1. The increased number of stimuli required for the longer scanning sessions (in our experiment, this limited the scan length);
2. The necessity for each baseline scan to be coupled to a specific activation scan and vice versa; and
3. The introduction of a working memory component into the task design by requiring the subject to switch tasks when presented with the prompt cue.

The coupling between activation and baseline tasks can be overcome, as indicated by Cherry et al. (*8*), by switching tasks in the activation scans only. This, however, would decrease the S/N gain (*8*). On the other hand, the memory component introduced by having to identify a cue to prompt task switching may limit the use of switched protocols in the study of memory or complex cognitive functions, as well as when patients with specific cognitive deficits are tested.

CONCLUSION

We investigated the effects of using a switched protocol for the identification of the neuronal areas activated during the execution of a higher-order cognitive task. We presented evidence suggesting that the switched protocol replicated the findings observed using rCBF imaging, yielded better S/N and did not introduce additional statistically significant foci although it involves an extra cognitive component. Switched protocols can be implemented easily and do not require extra personnel. However, the memory component introduced to switch tasks may limit the use of switched protocols when memory or other complex cognitive processes are studied.

ACKNOWLEDGMENTS

This work was supported by the Medical Research Council of Canada, grants SP-30, MT11541 and MT2624, and the McDonnell-Pew Program in Cognitive Neuroscience. We thank Pierre Ahad for his help in the preparation of the auditory stimuli, Dr. Keith Worsley for his suggestions regarding the statistical analysis of the data and the staff of the McConnell Brain Imaging Center for their technical assistance.

REFERENCES

1. Roland PE. *Brain activation*. New York: Wiley–Liss Inc.; 1993.
2. Mazziotta JC, Phelps ME. Positron emission tomography studies of the brain. In: Phelps ME, Mazziotta JC, Schelbert HR, eds. *Positron emission tomography and autoradiography. Principles and applications for the brain and heart.* New York: Raven Press; 1986:493–579.
3. Kanno I, Iida H, Miura S, Murakami M. Optimal scan time of oxygen-15-labeled water injection method for measurements of cerebral blood flow. *J Nucl Med* 1991;32:1931–1934.
4. Mintun MA, Raichle ME, Quarles RP. Length of PET data acquisition inversely affects ability to detect focal areas of brain activation. *J Cereb Blood Flow Metab* 1989; 9(suppl 1):S349.
5. Fox PT, Mintun MA, Reiman EM, Raichle ME. Enhanced detection of focal brain responses using intersubject averaging and change-distribution analysis of subtracted PET images. *J Cereb Blood Flow Metab* 1988;8:642–653.
6. Herscovitch P, Markham J, Raichle ME. Blood flow measured with intravenous $H_2{}^{15}O$. I. Theory and error analysis. *J Nucl Med* 1983;24:782–789.
7. Raichle ME, Martin WRW, Herscovitch P, Mintun MA, Markham J. Brain blood flow measured with intravenous $H_2{}^{15}O$. II. Implementation and validation. *J Nucl Med* 1983;24:790–798.
8. Cherry SR, Woods RP, Doshi NK, Banerjee PK, Mazziotta JC. Improved signal-to-noise in PET activation studies using switched paradigms. *J Nucl Med* 1995;36:307–314.
9. Vafaee M, Murase K, Gjedde A, Meyer E. Dispersion correction for automatic sampling of O-15-labeled H_2O and red blood cells. In: Myers R, Cunningham V, Bailey D, Jones T, eds. *Quantification of brain function using PET.* San Diego: Academic Press Inc.; 1996:72–75.
10. Kety SS. The theory and application of the exchange of inert gas at the lungs and tissues. *Pharmacol Rev* 1951;3:1–41.
11. Volkow ND, Mullani N, Gould LK, Adler SS, Gatley SJ. Sensitivity of measurements of regional brain activation with oxygen-15-water and PET to time of stimulation and period of image reconstruction. *J Nucl Med* 1991;32:58–61.
12. Raichle ME, Fiez VA, Videen TO, et al. Practice-related changes in human brain functional anatomy during nonmotor learning. *Cerebr Cortex* 1994;4:8–26.
13. Meyer E, Ferguson SS, Zatorre RJ, et al. Attention modulates somatosensory cerebral blood flow response to vibrotactile stimulation as measured by positron emission tomography. *Ann Neurol* 1991;29:440–443.
14. Klein D, Milner B, Zatorre RJ, Meyer E, Evans AC. The neural substrates underlying word generation: a bilingual functional imaging study. *Proc Natl Acad Sci USA* 1995;92:2899–2903.
15. Klein D, Zatorre RJ, Milner B, Johnsrude IS, Nikelski J, Meyer E, Evans AC. CBF patterns during synonym generation: group vs. individual study. *Neuroimage* 1996; 3(suppl):S444.
16. Evans AC, Thompson CJ, Marret S, Meyer E, Mazza M. Performance characteristics of the PC-2048: a new 15-slice encoded-crystal PET scanner for neurological studies. *IEEE Trans Med Imaging* 1991;10:90–98.
17. Votaw JR. Signal-to-noise ratio in neuro activation PET studies. *IEEE Trans Med Imaging* 1996;15:197–205.
18. Evans AC, Marret S, Neelin P, et al. Anatomical mapping of functional activation in stereotactic coordinate space. *Neuroimage* 1992;1:43–53.
19. Talairach J, Tournoux P. *Co-planar stereotaxic atlas of the human brain.* New York: Thieme Medical Publishers; 1988.
20. Evans AC, Marret S, Torrescorzo J, Ku S, Collins L. MRI-PET correlation in three dimensions using a volume-of-interest (VOI) atlas. *J Cereb Blood Flow Metab* 1991;11:A69–A78.
21. Worsley KJ, Evans AC, Marret S, Neelin P. A three-dimensional statistical analysis for CBF activation studies in human brain. *J Cereb Blood Flow Metab* 1992;12:900–918.
22. Petersen SE, Fox PT, Posner MI, Mintun M, Raichle ME. Positron emission tomographic studies of the cortical anatomy of single-word processing. *Nature* 1988;331:585–589.
23. McCarthy G, Blamire AM, Rothman DL, Gruetter R, Shulman RG. Echo-planar magnetic resonance imaging studies of frontal cortex activation during word generation in humans. *Proc Natl Acad Sci USA* 1993;90:4952–4956.
24. Petrides M, Alivisatos B, Meyer E, Evans A. Functional activation of the human frontal cortex during the performance of verbal working memory tasks. *Proc Natl Acad Sci USA* 1992;90:878–882.
25. Petrides M, Pandya DN. Comparative architectonic analysis of the human and the macaque frontal cortex. In: Boller F, Grafman J, eds. *Handbook of neuropsychology*, Vol. 9. Amsterdam: Elsevier Science; 1994:17–58.
26. Mintun MA, Fox PT, Raichle ME. A highly accurate method of localizing regions of neuronal activation in the human brain with positron emission tomography. *J Nucl Med* 1989;9:96–103.